IEEE Access
Multidisciplinary | Rapid Review | Open Access Journal

Received October 4, 2018, accepted December 6, 2018, date of publication January 10, 2019, date of current version February 4, 2019.

Digital Object Identifier 10.1109/ACCESS.2019.2891728

CPW Fed Wideband Corner Bent Antenna for 5G Mobile Terminals

G. S. KARTHIKEYA, (Student Member, IEEE), MAHESH P. ABEGAONKAR, (Senior Member, IEEE), AND SHIBAN K. KOUL, (Fellow, IEEE)

Centre for Applied Research in Electronics, IIT Delhi, New Delhi 110016, India

Corresponding author: Mahesh P. Abegaonkar (mpjosh@care.iitd.ac.in)

ABSTRACT A co-planar waveguide fed slot antenna element with 34% impedance bandwidth and 2–3 dBi broadside gain is proposed. The corner bent topology of the element is investigated for reduced physical footprint and easier integration with the mobile terminals operating in the 28-GHz band. The front-to-back ratio of the corner bent antenna is 1 dB in the *xy* plane, which indicates a high specific absorption rate. A compact wideband reflector is proposed which has transmission of less than −25 dB and a linear phase ±90° in the 27–33-GHz bandwidth. The wideband reflector is integrated with the corner bent antenna at 0.135λ offset from the radiating aperture. The corner bent antenna integrated with the reflector operates in the 27–33-GHz band, with a front-to-back ratio of more than 14 dB across the band and a forward gain of 6–7.2 dBi. The radiation patterns are stable for 20% bandwidth. The simulated and measured results are presented.

INDEX TERMS CPW fed antenna, 28 GHz corner bent antenna, 5G mobile terminal, wideband.

I. INTRODUCTION

Due to massive explosion in bandwidth hungry applications of cellular telephony, the hardware architecture for the future 5G communication system needs to support the proposed mmWave bands [1]. The candidate bands for 5G cellular telephony include 28 GHz and 37-40 GHz bands as proposed in [2]. The strategy is to ease spectral congestion in the sub-6 GHz bands. Hence, migration to higher carrier frequencies would facilitate design and development of hardware ecosystem compliant with the proposed bands [3]. The challenge with 28 GHz band deployment is the high path loss and penetration losses as reported in [4]. In order to compensate these, antennas deployed in the communication system need to mitigate their effects [3]. High gain necessarily means that the beamwidth would be low, hence decreasing coverage. It's a trade-off between gain and coverage area, which needs to be considered for design and deployment [5]. The desired characteristics of a 5G mobile terminal antenna include conformal structure, low physical footprint, high impedance bandwidth to support future spectrum at 28 GHz, stable patterns over the entire band with low specific absorption rate, high gain for the available aperture on the terminal and pattern diversity to support functionalities in multi-orientation [6]. Various configurations of antennas for 5G mobile terminals have been investigated such as [7] which has multilayered design, hence occupying relatively larger area, with a 9% impedance bandwidth. Even though the antenna element proposed in [8] has a 10% bandwidth the radiation patterns might not be suitable for integration with the mobile terminal. The element proposed in [9] has a bandwidth of more than 35% with an end fire gain of 4-6 dBi, but the design is planar. The design presented in [10] offers 20% bandwidth with a SIW feed, hence increasing the complexity of the design. It must be noted that most of the reported designs are planar and designed with microstrip feed.

Conformal designs have been proposed earlier, such as in [11] meant for lightweight UAV applications, the design process could be adapted for a mobile terminal but the scaffolding of antenna would contribute to losses in addition to impedance mismatch. The SIW conformal antenna proposed in [12] would increase the complexity of fabrication process. The conformal antenna proposed in [13] is designed at 60 GHz and mounted on a cylindrical surface with a radius of 25 mm, hindering its utility in 5G mobile terminals at 28 GHz. CPW feed would be the preferred method of feeding conformal antennas to be integrated with mobile terminals to facilitate uniplanar transition.

CPW feed is feasible at lower frequencies upto 15 GHz as demonstrated in [14], the dimensions of the 50Ω feed line would permit the application of standard inexpensive chemical etching process for fabrication. The CPW feed is also popular at mmWave frequencies and beyond since the dimensions of the transmission line would be readily feasible with the micro-fabrication technologies [15].

The CPW fed LPDA antenna proposed in [16] has a gain of 1.5 - 4 dBi and is planar in nature. Even though, the CPW-fed mmWave antenna demonstrated in [17] has an operating frequency at 30 GHz, the bandwidth is low (less than 5%) and it uses an air-bridge in the feedline for impedance match. Hence, a wideband CPW-fed corner bent antenna is proposed. The proposed antenna has low physical footprint and stable patterns in the 27 to 33 GHz band with a forward gain of 6-7 dBi. Detailed designs, simulation and measurement results are presented. The proposed CPW fed slot antenna is described in section II, followed by its corner bent counterpart in section III. The corner bent antenna backed by wideband reflector is described in section IV.

II. CPW FED WIDEBAND ANTENNA

The proposed CPW fed slot antenna is illustrated in Figure 1. It is constructed on Nelco NY9220 substrate with ε_r of 2.2 and 0.508 mm thickness. A low dielectric constant is chosen to keep the surface wave modes to a minimum as opposed to a higher dielectric constant substrate [16]. Electrically thin substrate was chosen to keep the cross-pol radiation to a minimum in the end fire. A 2.7mm wide CPW line with a gap of 0.2mm is chosen for the feed line since wider trace lines larger than half wavelength at the frequency of interest would lead to an over-moded antenna and hence results in dual-beam with poor patterns in the broadside [19].

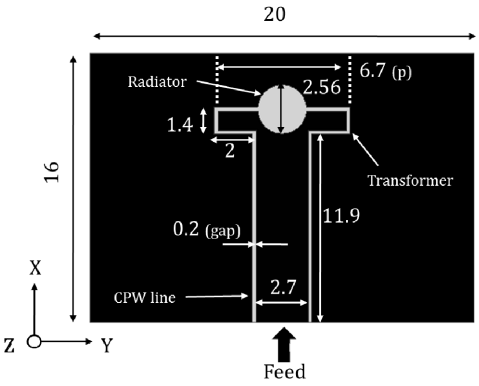

FIGURE 1. CPW fed wideband slot antenna design (all dimensions in mm).

The circular slot is the primary radiator in this topology. The feed is a 59Ω CPW line in series with a stepped impedance transformer of 50Ω followed by the capacitive slot, which has a high impedance of around 80 Ω leading to an input impedance of around 65Ω, hence achieving $|S_{11}|$ less than -10dB.

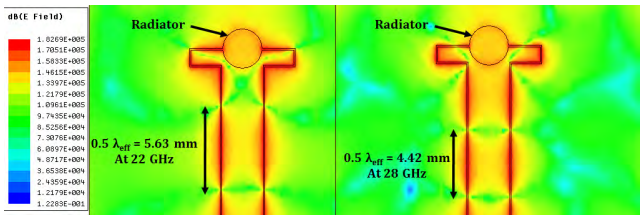

FIGURE 2. E field plot at 22 and 28 GHz.

Figure 2 illustrates the E field patterns at 22 and 28 GHz of the proposed antenna, the half-wavelength transmission mode is also illustrated. It is observed that the circular slot is uniformly illuminated irrespective of the frequency, hence a wide impedance bandwidth is achieved.

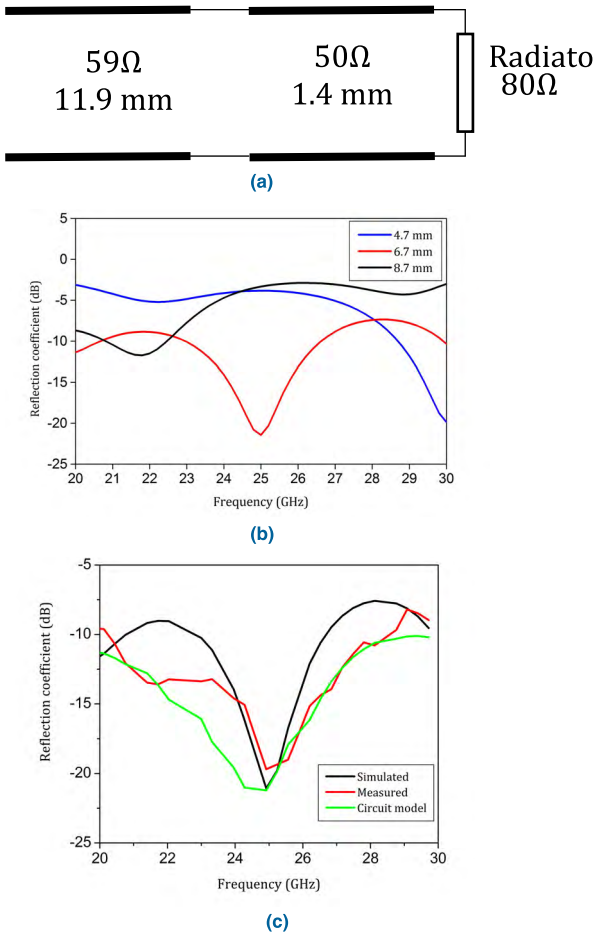

FIGURE 3. (a) Equivalent circuit of the proposed element. (b) Reflection coefficient variation with p. (c) Reflection coefficient of the proposed CPW fed antenna.

The equivalent circuit is shown in Figure 3(a) and this was simulated in Agilent ADS. The diameter of the radiating slot matches quarter-wavelength at 28 GHz. An impedance match at the lower end of the frequency range could be achieved with a diameter tuning near 2 mm. The distance between the feed and the radiating aperture is maintained at more than 1λ to reduce mutual coupling between the

end-launch connector and the antenna [21]. The overall width is sufficient for the connector mount and to maintain broadside patterns. The T shaped transformer is key for achieving the impedance match over more than 30% of the bandwidth. The input reflection coefficient variation with width of the stepped impedance transformer (p) is shown in Figure 3(b). For the chosen quarter-wave aperture dimension and the CPW feed line, the optimal width of the transformer was found to be 6.7 mm. The contour of the slot is equally important to establish the impedance match and beam integrity. For instance, square or elliptical slots would result in less than 15% bandwidth due to improper mode excitations.

Since, the radiating aperture is not backed by a ground plane, a symmetric beam is formed on both sides of the aperture [15]. The simulated and measured input reflection coefficient is depicted in Figure 3(c). All the full-wave simulations were performed in Ansys HFSS. The measured impedance bandwidth is from 20 to 28 GHz (34%). The variation in input reflection coefficient is minimal even with a gap of upto 0.3mm in the CPW feedline. The measurements were done using Agilent PNA E8364C. The discrepancy could be attributed to fabrication tolerances, and the deviation between port impedance used in simulation and the impedance offered by the end-launch connector. A multi-segmented impedance transformer would have resulted in higher bandwidth, with a re-designed profile of the radiator, but the broadside patterns would be more specular.

The radiation patterns in both the principal planes i.e., E plane (XZ plane) and H plane (YZ plane) at 22, 25 and 28 GHz are shown in Figure 4. The front to back ratio is almost 0 dB. The deviations between simulated and measured patterns is due to alignment errors and adapters utilized for measurements in the anechoic chamber.

The broadside gain is illustrated in Figure 5. The simulated gain varies from 2 to 3 dBi across the bandwidth. Since, the measured beamwidths in the H plane (YZ) are more than 50° across the band, a low but consistent gain has been observed. Gain measurements were performed with the standard gain transfer method using Keysight horn antennas [22]. It must be noted that to mitigate the path loss at 28 GHz, high gain antennas must be incorporated in the mobile terminals.

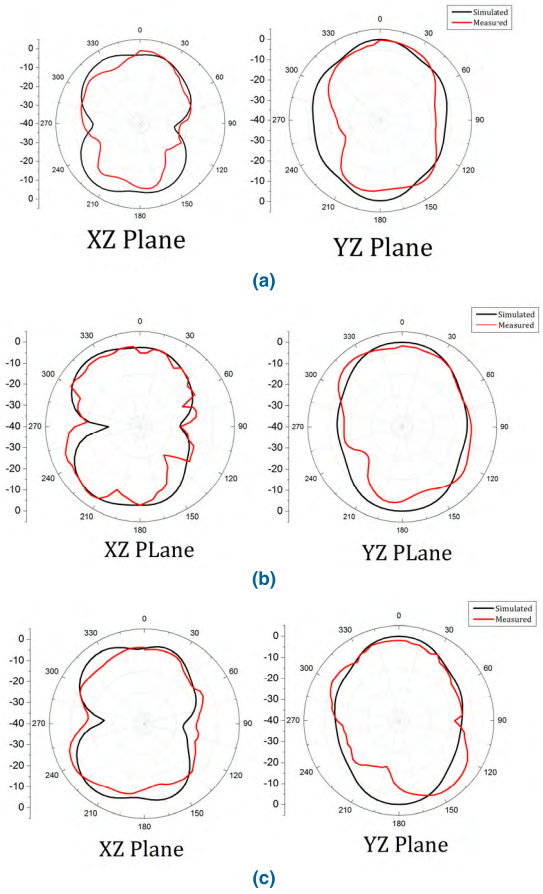

FIGURE 4. Patterns in XZ and YZ planes at (a) 22 GHz (b) 25 GHz and (c) 28 GHz.

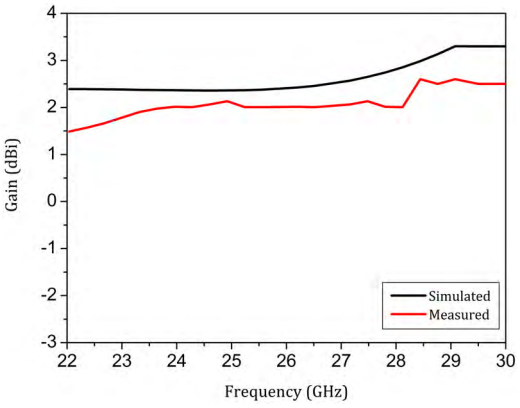

FIGURE 5. Broadside gain of the proposed antenna.

III. CPW FED CORNER BENT ANTENNA

The proposed antenna occupies electrically large volume ($1.6\lambda \times 2\lambda$), hence might be unsuitable for mobile terminals as it is. Hence, a corner bent architecture is proposed. The CPW fed slot antenna is bent before the stepped impedance transformer, to create a uniform illumination towards the base station. But due to lack of a ground plane, the beam is split towards and away from the base station. The choice of 20 mil substrate is justified due its structural stability even after the introduction of the discontinuity. 5 to 10 mil substrates would be an ideal choice for corner bent architecture, but the dielectric scaffolding on which the antenna would be supported would create an additional detuning of the antenna [11]. Substrates beyond 30 mil would be much more stable structurally but the antenna would have to be built in a piece-wise manner, hence creating a substantial discontinuity in the feed-line leading to significant distortions in the radiation patterns.

It must also be noted that uniplanar feed would create the least discontinuity when the radiating structure is conformed onto the mobile terminal. Conventional microstrip feed would lead to increased discontinuity in the ground plane, as the

17μm of Copper on the ground plane is exposed to more strain, hence leading to higher fracture of the copper trace leading to poor transition to the radiator.

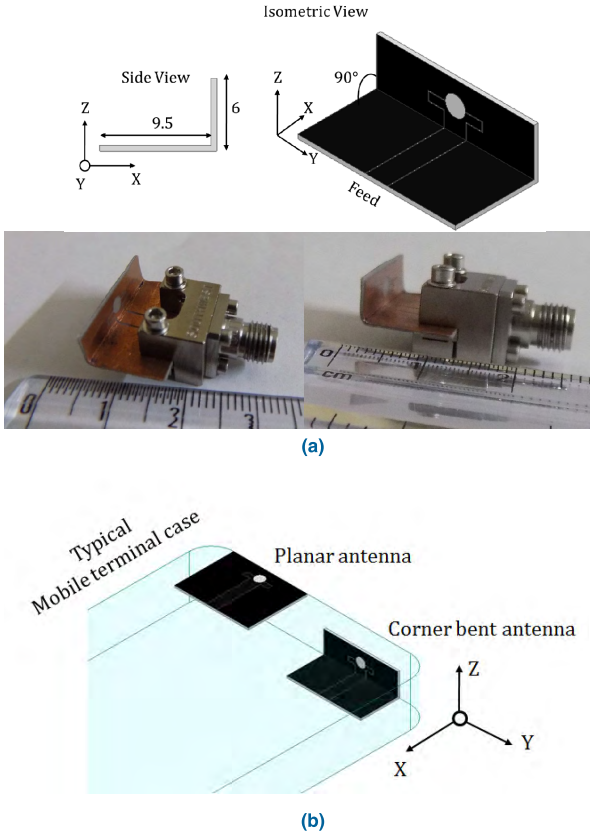

FIGURE 6. (a) CPW fed corner bent antenna with photographs. (b) Comparison of antennas on a mobile terminal.

The corner bent antenna design is illustrated in Figure 6(a). The radiating aperture was maintained with a clearance away from the orthogonal ground to create a reasonable beam on both sides in the XY plane.

The distance between the feed and the aperture is still at 1λ to facilitate good radiation pattern measurements with the end launch connector [21]. It is evident from Figure 6(b) that the radiation from a conventional antenna would be directed towards the user when in use. The proposed topology occupies lesser volume compared to the planar design.

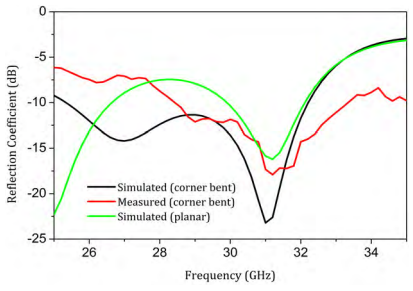

FIGURE 7. Reflection coefficient of corner bent antenna.

The simulated and measured input reflection coefficient of the corner bent antenna is shown in Figure 7. The measured impedance bandwidth is from 28.5 to 33.5 GHz that is 16.2%. The reduction in impedance bandwidth is due to the introduction of discontinuity. The discrepancy between simulated and measured curves is due to the non-ideal bending of the 20 mil copper clad dielectric. Also, the corner bent model was assumed to incorporate a perfect 90° bend in simulation, but a minor alignment error would have crept-in the implementation of the antenna.

The reflection coefficient deviation from the planar and corner bent design could be reduced with a CPW fed LPDA [16], but achieving uniform gain for more than 20% bandwidth might be a challenging task. To maintain the input impedance behavior of the planar and its corner bent counterpart, additional impedance transformer could be designed, but since the reflection coefficient is within acceptable limits for the frequency of interest, additional design tweak was not necessary. The inductive corner bent discontinuity creates an input impedance of (42-j11) Ω and (61+j7) Ω at 27 GHz and 31 GHz hence creating a dual mode of operation, but the $|S_{11}| < -10$ dB for a wider band.

The E-plane (XZ plane) co-pol and cross-pol patterns are shown in Figure 8(a) from 27 to 30 GHz, in steps of 1GHz. The measured front beamwidth is around 25° ± 10° and front to back ratio of 0.5dB in the E-plane. The front half-space is primarily due to the radiating slot, the radiation on the other side is due to the scattering effects from the electrically large ground in the orthogonal direction. It must also be observed that the effective aperture has been increased in the E-plane due to the parasitic ground, resulting in a decrease of beamwidth compared to the planar design, consequently increasing the gain by almost 2 dB in the bandwidth of interest. The H-plane (XY plane) patterns are shown in Figure 8(b). Since, the parasitic ground plane is in the orthogonal plane, it has minimal influence on the H-plane patterns. The front beamwidth is around 60° ± 10° with a front to back ratio of 1 dB illustrating that the beam is almost identically split, with slightly higher radiation in the forward direction compared to the radiation towards the user, when mounted on a mobile terminal.

The measured patterns have a deviation in the back-lobe due to utilization of the electrically large adapter for pattern measurements. The forward gain in the XY plane varies from 4 to 5.6 dBi in the span from 25 to 33 GHz. measured gain is also depicted in Figure 9. Since, the gain is stable across 27.5% bandwidth, the proposed corner bent antenna could be used for the 5G mobile terminals. The radiation patterns of the corner bent antenna illustrates that energy is directed towards the base station and the user. The proposed topology would also lead to higher specific absorption rate. In order to mitigate this effect, the back lobe must be diminished and enhance gain towards base station.

Several techniques could be incorporated for reduction of back lobe: A localized ground plane could be designed which would essentially be effective for a narrowband. An absorber such as Salisbury screen could be placed at quarter-wavelength away from the radiating aperture, but the

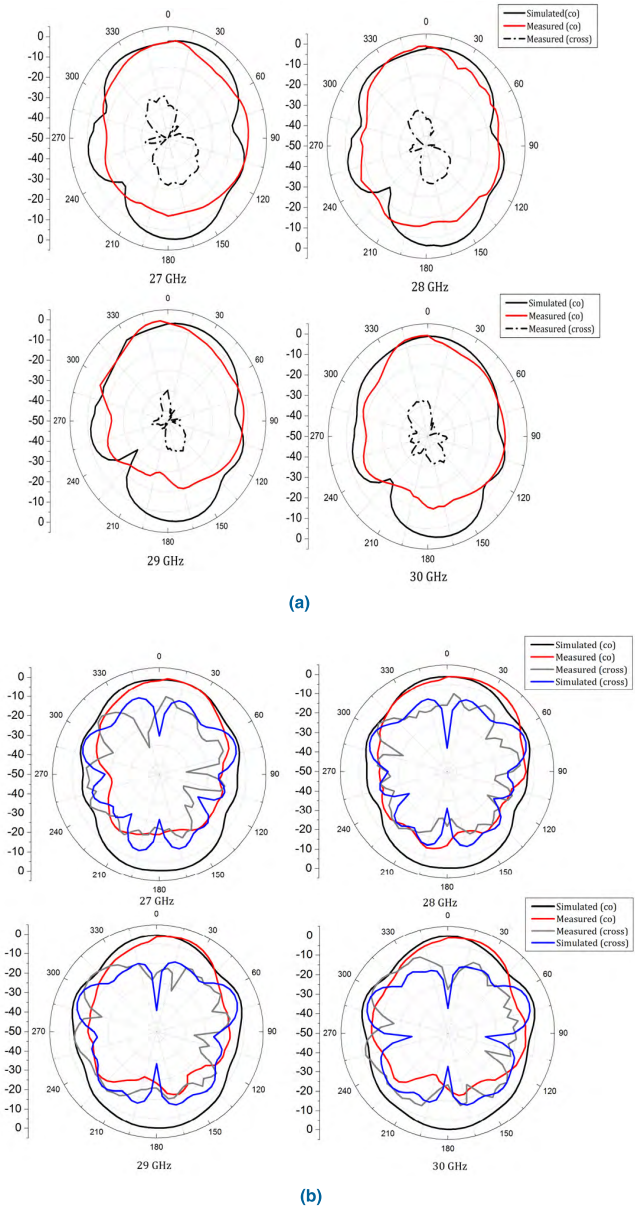

FIGURE 8. (a) Patterns in XZ plane at 27-30 GHz. (b) Patterns in XY plane at 27-30 GHz.

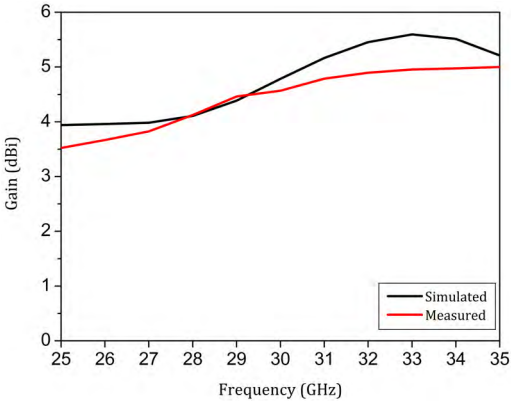

FIGURE 9. Forward gain of the corner bent antenna.

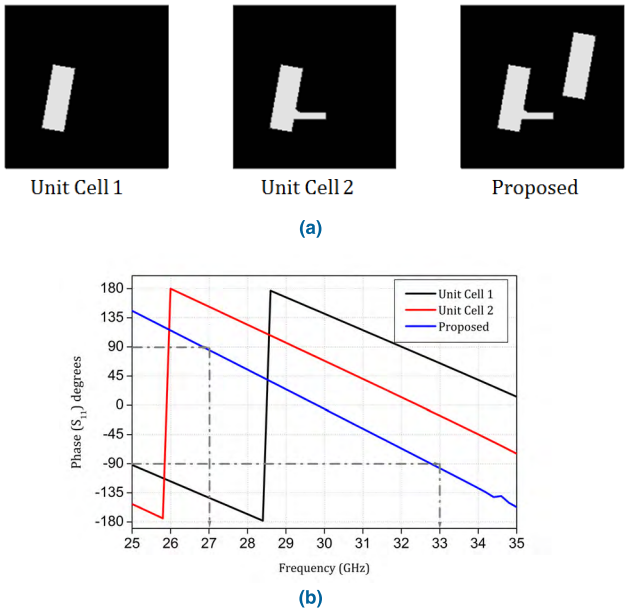

FIGURE 10. (a) Design evolution of the unit cell. (b) Input phase response of the unit cells.

gain would be reduced. The third technique is to place a wideband reflector for back-lobe reduction leading to gain enhancement in the forward direction [24], since this architecture would provide relatively higher gain for a wider band compared to other methods, the reflector design is investigated.

IV. CORNER BENT ANTENNA WITH REFLECTOR

The obvious solution for design of a reflector would be to mount an electrically large (atleast $3\lambda \times 3\lambda$) metal behind the radiating aperture at quarter-wavelength at the center frequency, but this topology decreases the impedance bandwidth, hence a wideband reflector with periodic structure is proposed. It must also be noted that if reflector size is 3λ, i.e., 30 mm at 28 GHz, this dimension would be unacceptable since the panel height of typical smartphones is 10-15 mm [6]. Hence, the antenna integrated with reflector must offer high impedance bandwidth, gain and compact size. A linear phase structure is essential for gain enhancement, hence the slots are strategically etched as shown in the design evolution schematics of Figure 10(a) the corresponding phase variation against frequency is illustrated in Figure 10(b). The proposed unit cell and the simulation model are shown in Figure 11(a). Conventional cross slots would be narrowband, the other alternative is to design multilayered reflectors to create a net effect of wideband reflection, and this topology would increase the overall size of the antenna. The overall size of the proposed unit cell is $0.5\lambda \times 0.5\lambda$ at 28 GHz. two slanted stubs are etched out from Copper on the top plane of Nelco NY9220 20 mil substrate. The topology yields a linear phase $\pm 90°$ in the frequency range of 27 to 33 GHz as depicted

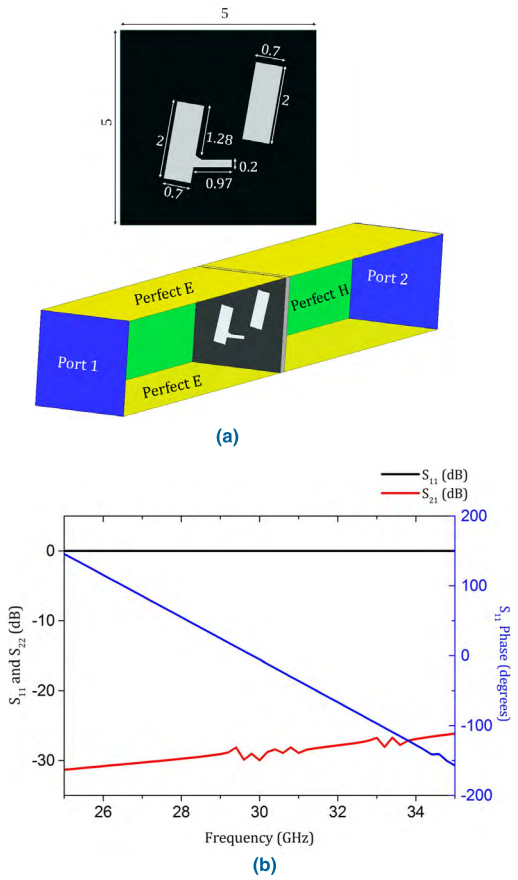

FIGURE 11. (a) Proposed unit cell with simulation model. (b) Simulated S_{11} and $|S_{21}|$ of the proposed unit cell.

in Figure 11(b). Periodic boundary conditions were used in simulations. The polarization of the incoming plane wave was identical to that of the antenna, also the length of the waveguide was optimized to support only the dominant mode of propagation. The transmission and reflection characteristics are also illustrated in Figure 11(b). $|S_{21}|$ is below -25 dB in the 25 to 35 GHz band. A 2×4 array of unit cells was designed as the reflector. This translates to $1\lambda \times 2\lambda$ at 28 GHz.

The reported designs of wideband reflectors have an aperture of more than $2\lambda\times2\lambda$. The height of the proposed reflector decides front to back ratio in the E-plane. It was a compromise between the pattern and the footprint of the antenna. The width of the reflector decides the H-plane pattern, and hence the forward gain. 1mm of offset is maintained between the CPW line and the reflector to prevent coupling. The proposed antenna backed by wideband reflector is illustrated in Figure 12(a).

The complete radiating structure is working in the quasi waveguide mode wherein the electrically small aperture radiates towards the reflector placed at 0.135λ which undergoes multiple reflections followed by radiation from the effective aperture as illustrated in Figure 12(b). The offset between the reflector and the radiating aperture is the critical parameter which decides the gain and impedance bandwidth. It is observed that when the reflector is electrically close to

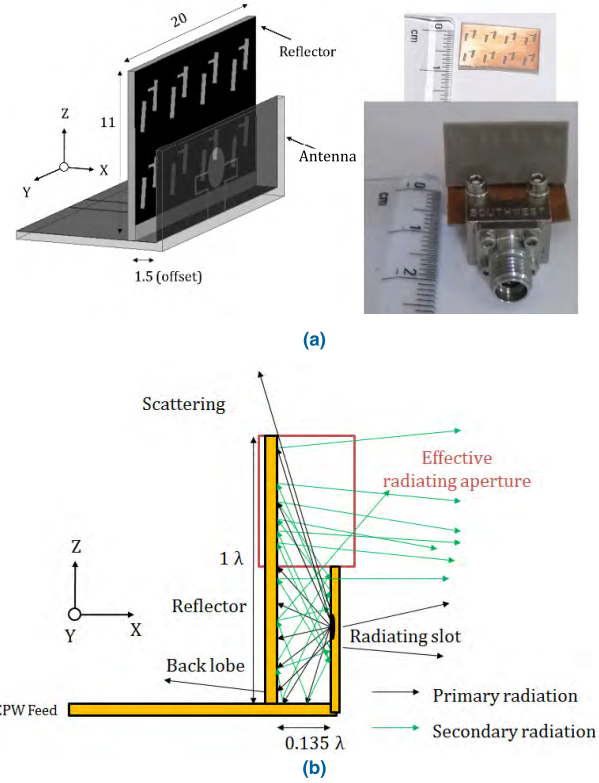

FIGURE 12. (a) Corner bent antenna with reflector design. (b) Field diagram of the radiation mechanism.

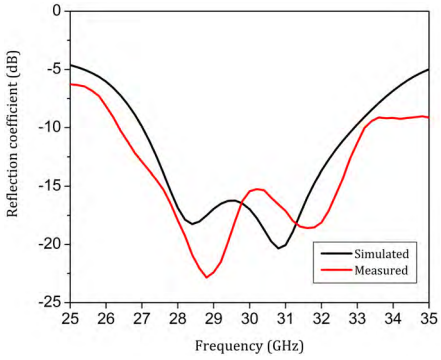

FIGURE 13. Reflection coefficient of corner bent antenna backed by wideband reflector.

the radiator, the reflector acts as the primary radiator and the slot becomes a parasitic, hence the antenna is strongly detuned, since the reflector does not support radiation per se. When the reflector is electrically far away from the slot (offset being 3 mm), the impedance bandwidth increases to 28% with a deterioration in gain. The offset of 1.5mm is chosen by considering the reflection coefficient and gain trade-off. A similar performance was observed when a PEC was substituted with similar aperture, but with an offset at 2 mm, hence proving that the proposed reflector is relatively compact. The simulated and measured reflection coefficient is depicted in Figure 13. The impedance bandwidth is from 27 to 33 GHz (20%). The slight discrepancy is due to non-ideal alignment between the reflector and radiator.

The reflector acts as a shunt admittance to the radiator hence, offering an input impedance of (39-j4) Ω and (49-j9) Ω at 28 GHz and 31 GHz respectively, but since the frequencies are close a wide impedance bandwidth is achieved.

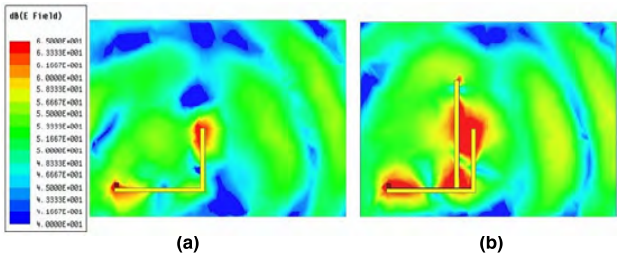

FIGURE 14. E-field plot of corner bent antenna (a) without and (b) With wideband reflector at 28 GHz.

Figure 14 illustrates the E-field plot of the side-view, without and with reflector of the corner bent antenna. The transmission mode of the CPW line and the radiation mode is clearly visible in both the plots. It must also be observed that without the reflector the orthogonal ground plane splits the beam in both the directions. The diffraction effect with the reflector is also clearly visible.

The experimental setup used in the measurements is depicted in Figure 15. The inset photograph shows the zoomed view of the antenna under test.

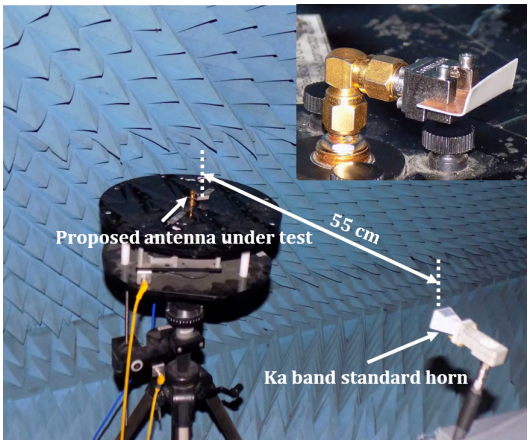

FIGURE 15. Experimental setup of radiation pattern measurement.

The simulated and measured co-pol and cross-pol patterns from 27 to 30 GHz are illustrated in Figure 16. The beamwidth in the E plane (XZ plane) is around 76° ± 5°. The decrease in beamwidth is due to the cavity effect of the reflector and the slot. The radiation patterns are stable for the entire 20% band. The front to back ratio is more than 12 dB, as against 1dB without the reflector. This ratio could be further improved with a larger effective aperture symmetrically, leading to an increase in the footprint of the antenna. These values prove the utility of the proposed antenna in reduction of specific absorption rate when integrated with a mobile terminal. The sidelobe at 190° to 220° is primarily due to the

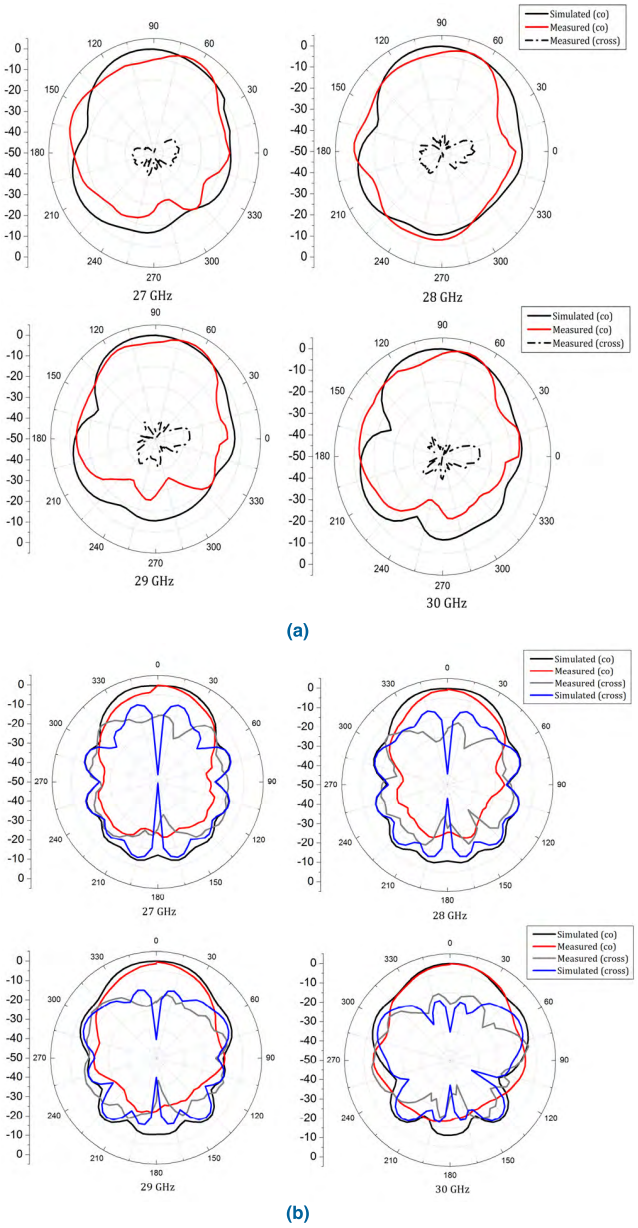

FIGURE 16. (a) Patterns in XZ plane at 27-30 GHz. (b) Patterns in XY plane at 27-30 GHz.

reduced aperture in the z-direction. The sidelobe suppression would increase the forward gain by 0.5dB, hence the aperture is compromised. An L bent reflector was also attempted to reduce the sidelobe but it led to increased scattering from the sides. The patterns in H plane (XY plane) have a beamwidth of 60° ± 50°. The front to back ratio is more than 14 dB for 20% bandwidth. Since the effective aperture of the reflector is 2λ in the H-plane, hence a reduced beamwidth and superior front to back ratio is observed. The beamwidth increases at the higher end of the band due to chosen offset length of 0.135λ.

The 3D patterns in Figure 17 provides an insight into the radiation without and with reflector at 28 GHz, the behavior is similar in the entire band.

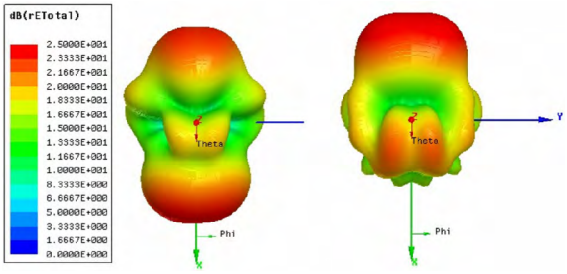

FIGURE 17. 3D Patterns without and with reflector at 28 GHz.

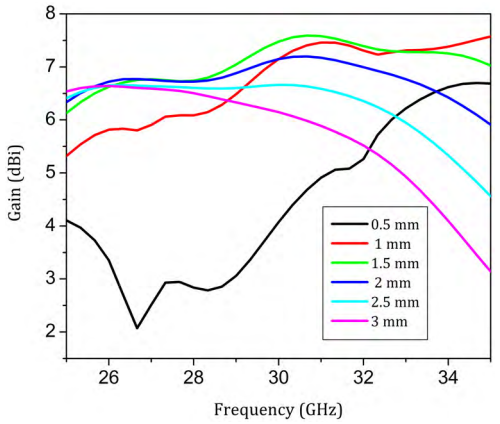

FIGURE 18. Simulated forward gain with parametric analysis.

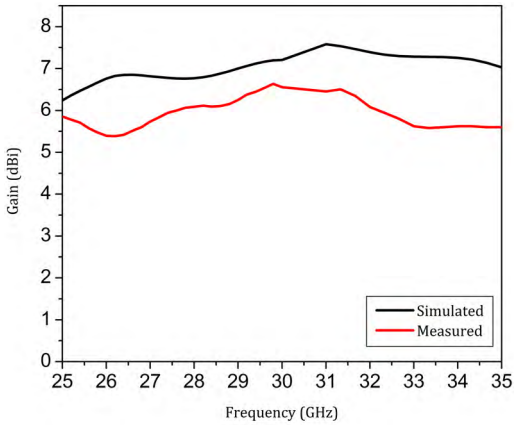

FIGURE 19. Forward gain of the corner bent antenna with reflector.

The forward gain is shown in Figure 18 with the offset parametric analysis. As it is observed the gain is highest when the reflector is offset at 1.5mm. The parametric analysis is also in accordance with the gain-bandwidth principle. Since, the increase in volume between the reflector and the radiating aperture leads to an increase in the impedance bandwidth and a consequent decrease in the gain [25]. Simulated gain varies from 6 to 7 dBi in the band 25 to 35 GHz. Stable patterns across the band resulted in stable gain in H-plane. The gain is comparable to a strongly resonant microstrip patch antenna.

Gain enhancement of almost 2 dB is observed across the 20% band. Ideally, the gain enhancement should have been 3dB but since the reflector aperture is compromised, the gain enhancement is deviated.

The simulated and measured gain curves are depicted in Figure 19. The maximum deviation between the two is 1.5dB.

The proposed designs along with the characteristics is summarized in Table 1.

TABLE 1. Proposed designs' summary.

Design	Impedance BW(GHz)	Gain (dBi)	Front to Back ratio (dB)
CPW fed (Planar)	20-28 (34%)	2-3	0
Corner bent	28.5-33.5 (16.2%)	4-5.6	1
Corner bent with reflector	27-33 (20%)	6-7	>12

The proposed CPW fed corner bent antenna integrated with a reflector has a wide impedance bandwidth with least gain variation compared to reported planar designs, as illustrated in Table 2.

TABLE 2. Comparison with other designs.

Ref.	Imp BW(GHz)	Gain (dBi)	Feed	Corner bent
[19]	24-28 (15%)	3-4.5	CPW	No
[20]	57-64 (11.6%)	8-9	Microstrip	No
[21]	22-24 (8.7%)	4-6	Microstrip	No
[22]	21-25 (17%)	8-10	CPS	No
Proposed	27-33 (20%)	6-7	CPW	Yes

V. CONCLUSION

A 20% wide impedance bandwidth antenna element with CPW feed on electrically thin substrate has been presented. The corner bent topology of the element has been investigated, which leads to minor detuning and poor front to back ratio due to the parasitic orthogonal ground plane. A wideband reflector is proposed and integrated with the corner bent radiator at 0.135λ to enhance front to back ratio upto 14 dB across the band. The impedance bandwidth is more than 20% with stable radiation patterns and forward gain of 6-7 dBi across the band of the proposed antenna.

REFERENCES

[1] *Cisco Visual Networking Index: Global Mobile Data Traffic Forecast Update 2009–2014*, Cisco Public Information, Forecast, Cisco VNI, Feb. 2010.
[2] C.-X. Wang *et al.*, "Cellular architecture and key technologies for 5G wireless communication networks," *IEEE Commun. Mag.*, vol. 52, no. 2, pp. 122–130, Feb. 2014.
[3] W. Hong, K.-H. Baek, Y. Lee, Y. Kim, and S.-T. Ko, "Study and prototyping of practically large-scale mmWave antenna systems for 5G cellular devices," *IEEE Commun. Mag.*, vol. 52, no. 9, pp. 63–69, Sep. 2014.
[4] T. S. Rappaport *et al.*, "Millimeter wave mobile communications for 5G cellular: It will work!" *IEEE Access* vol. 1, pp. 335–349, 2013.

[5] J. Zhang, X. Ge, Q. Li, M. Guizani, and Y. Zhang, "5G millimeter-wave antenna array: Design and challenges," *IEEE Wireless Commun.*, vol. 24, no. 2, pp. 106–112, Apr. 2017.
[6] C. Rowell and E. Y. Lam, "Mobile-phone antenna design," *IEEE Antennas Propag. Mag.*, vol. 54, no. 4, pp. 14–34, Aug. 2012.
[7] O. M. Haraz, A. Elboushi, S. A. Alshebeili, and A.-R. Sebak, "Dense dielectric patch array antenna with improved radiation characteristics using EBG ground structure and dielectric superstrate for future 5G cellular networks," *IEEE Access* vol. 2, pp. 909–913, 2014.
[8] J.-S. Park, J.-B. Ko, H.-K. Kwon, B.-S. Kang, B. Park, and D. Kim, "A tilted combined beam antenna for 5G communications using a 28-GHz band," *IEEE Antennas Wireless Propag. Lett.*, vol. 15, pp. 1685–1688, 2016.
[9] S. X. Ta, H. Choo, and I. Park, "Broadband printed-dipole antenna and its arrays for 5G applications," *IEEE Antennas Wireless Propag. Lett.*, vol. 16, pp. 2183–2186, 2017.
[10] P. Choubey, W. Hong, Z.-C. Hao, P. Chen, T.-V. Duong, and M. Jiang, "A wideband dual-mode SIW cavity-backed triangular-complimentary-split-ring-slot (TCSRS) antenna," *IEEE Trans. Antennas Propag.*, vol. 64, no. 6, pp. 2541–2545, 2016.
[11] K. Sarabandi, J. Oh, L. Pierce, K. Shivakumar, and S. Lingaiah, "Lightweight, conformal antennas for robotic flapping flyers," *IEEE Antennas Propag. Mag.*, vol. 56, no. 6, pp. 29–40, Dec. 2014.
[12] Y. J. Cheng, H. Xu, D. Ma, J. Wu, L. Wang, and Y. Fan, "Millimeter-wave shaped-beam substrate integrated conformal array antenna," *IEEE Trans. Antennas Propag.*, vol. 61, no. 9, pp. 4558–4566, Sep. 2013.
[13] V. Semkin *et al.*, "Beam switching conformal antenna array for mm-wave communications," *IEEE Antennas Wireless Propag. Lett.*, vol. 15, pp. 28–31, 2016.
[14] L.-M. Si, W. Zhu, and H.-J. Sun, "A compact, planar, and CPW-fed metamaterial-inspired dual-band antenna," *IEEE Antennas Wireless Propag. Lett.*, vol. 12, pp. 305–308, 2013.
[15] S. Raman and G. M. Rebeiz, "94 GHz slot-ring antennas for monopulse applications," in *Antennas Propag. Soc. Int. Symp. Dig.*, vol. 1, Jun. 1995, pp. 722–725.
[16] G. Zhai, Y. Cheng, Q. Yin, S. Zhu, and J. Gao, "Uniplanar millimeter-wave log-periodic dipole array antenna fed by coplanar waveguide," *Int. J. Antennas Propag.*, vol. 2013, Sep. 2013, Art. no. 430618.
[17] D. M. Elsheakh and M. F. Iskander, "Circularly polarized triband printed quasi-Yagi antenna for millimeter-wave applications," *Int. J. Antennas Propag.*, vol. 2015, Jan. 2015, Art. no. 329453.
[18] R. W. Jackson, "Considerations in the use of coplanar waveguide for millimeter-wave integrated circuits," *IEEE Trans. Microw. Theory Techn.*, vol. MTT-34, no. 12, pp. 1450–1456, Dec. 1986.
[19] S. F. Jilani, S. M. Abbas, K. P. Esselle, and A. Alomainy, "Millimeter-wave frequency reconfigurable T-shaped antenna for 5G networks," in *Proc. IEEE 11th Int. Conf. Wireless Mobile Comput., Netw. Commun. (WiMob)*, Oct. 2015, pp. 100–102.
[20] A. Dadgarpour, B. Zarghooni, B. S. Virdee, and T. A. Denidni, "Single end-fire antenna for dual-beam and broad beamwidth operation at 60 GHz by artificially modifying the permittivity of the antenna substrate," *IEEE Trans. Antennas Propag.*, vol. 64, no. 9, pp. 4068–4073, Sep. 2016.
[21] R. A. Alhalabi and G. M. Rebeiz, "High-efficiency angled-dipole antennas for millimeter-wave phased array applications," *IEEE Trans. Antennas Propag.*, vol. 56, no. 10, pp. 3136–3142, Oct. 2008.
[22] R. A. Alhalabi and G. M. Rebeiz, "Differentially-fed millimeter-wave Yagi-Uda antennas with folded dipole feed," *IEEE Trans. Antennas Propag.*, vol. 58, no. 3, pp. 966–969, Mar. 2010.
[23] T. Girard, R. Staraj, and E. Cambiaggio, "Conformal microstrip antenna arrays fed by bent coplanar waveguides," *Electron. Lett.*, vol. 34, no. 3, pp. 226–227, Feb. 1998.
[24] K. Ding, C. Gao, T. Yu, and D. Qu, "Wideband CP slot antenna with backed FSS reflector," *IET Microw., Antennas Propag.*, vol. 11, no. 7, pp. 1045–1050, Jun. 2017.
[25] R. Garg, *Microstrip Antenna Design Handbook*. Norwood, MA, USA: Artech House, 2001.

Authors' photographs and biographies not available at the time of publication.